Developments in NWP system and Satellite Data Assimilation at DWD

Deutscher Wetterdienst
Wetter und Klima aus einer Hand

Ch. Köpken-Watts, R. Faulwetter, O. Stiller, A. Fernandez del Rio, S. Hollborn, A. Walter,
S. May, K. Raykova, L. Bach (SAT); A. Rhodin, H. Anlauf (DA)

I) Operational NWP system & satellite usage

Global:
- **ICON @ 13 km global / 6.5 km Europe** (two-way nest within global runs)
- **EnVar ensemble DA**, 40 members @ 40/20 km (global/Europe), **see II**
- **ICON – EPS global ensemble forecasts** @ 40/20 km (operational Dec 2017)

High-resolution:
- **COSMO-DE: 2.8 km**, 50 levels (non-hydrostatic)
- **KENDA (LETKF) ensemble DA**, 40 members @ 2.8 km with latent heat nudging (LHN) for radar precipitation
- **COSMO-DE-EPS ensemble forecasts @ 2.8 km**, 40 members

Satellite data/ global ICON:
- AMSU-A (chan 9-14 everywhere, 5-8 only over sea), ATMS (similar, 3*3 superobbing)
- HIRS (chan 4-7, 14, 15, over sea), IASI (45 chan, McNally&Watts cloud detection, over sea)
- GPS-RO bending angles
- AMVs (GEO, LEO), ASCAT winds
- MHS & IASI humidity channels pre-operational (for Q1/2018, **see III**)
- Monitoring: further MW-Sounders & Imagers implemented (**see III**), CrIS, Meteosat CSR, Jason-2/3 winds

Technical aspects:
- RTTOV-10 (update to RTTOV-12 for Q1/2018)
- Online bias correction
- Flexible satellite pre-processing & monitoring auto-alert packages

Current developments:
- Extended IASI usage, introduction of CrIS
- Operational introduction of VarBC
- MW and IR surface sensitive radiances (**see IV**)
- Use of IASI PC compressed data (**see V**)
- SEVIRI cloudy radiances (infrared water vapour and visible, **see VI**)
- Observation impact diagnostics in ensemble DA (see **Poster 12p.09**)

II) Operational Introduction of Ensemble DA

A fundamental upgrade of DWD's operational NWP system has taken place over the last three years, consisting of:

1) Global model ICON model (**ICO**sahedral **N**on-hydrostatic modelling framework, developed in cooperation between DWD and the MPI Hamburg for climate research), operational since **January 2015**. The non-hydrostatic model is formulated on an **icosahedral grid,** runs currently at **13km** resolution with **90 vertical σ-z-levels** (model top at 70km/~2.6 Pa). Higher resolution forecasts are provided at **6.5 km for a European domain** using two-way nesting (ICON-EU, see Fig. 1).

2) Global EnVAR data assimilation, operational since **January 2016**: A global LETKF ensemble data assimilation (following Hunt et al. 2007) at lower resolution, providing flow dependent background errors, is coupled to a full resolution deterministic 3DVar. The current ensemble size is 40 members (to be increased in 2018). See **Fig 1.** for schematic illustration of the setup.

3) Global ensemble forecasts, the **ICON-EPS,** with 40 members based on the analysis ensemble will become operational in **December 2017** and produce forecasts up to 120 h (00, 12 UTC) and additionally 3-hourly 24 h forecasts used as boundaries for the regional ensemble.

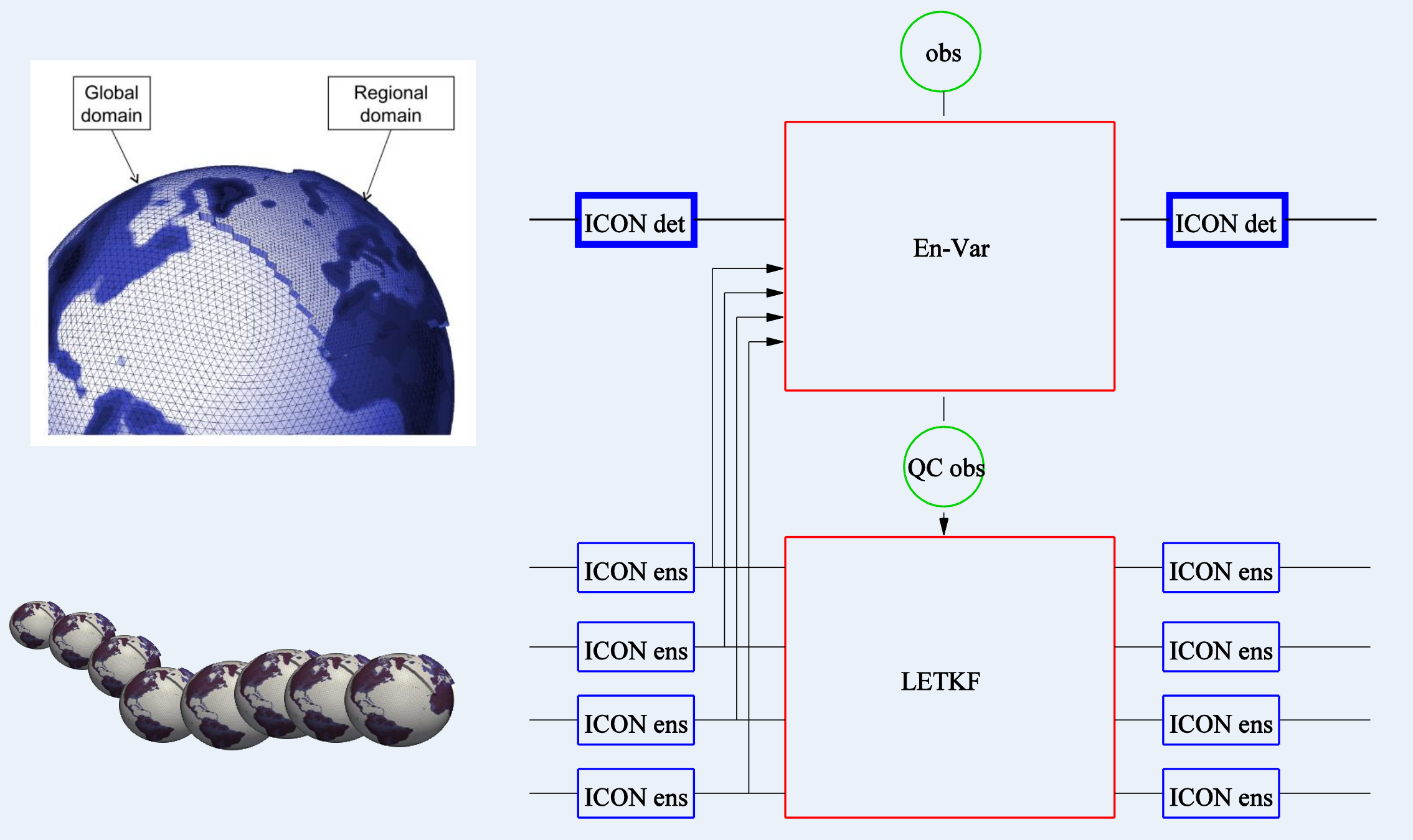

Fig 1: Schematic diagram of the global NWP system: Interaction between global ensemble prediction (ICON ens, 40 km global/20 km Europe nest resolution) using LETKF ensemble analysis and the higher resolution deterministic forecast (ICON det, 13 km global/6.5 km Europe) using the EnVar analysis. The EnVar uses the flow-dependent background errors from the ensemble blended with climatological covariances (70% ensemble B and 30% climatological B). The observation processing and quality control (QC) are performed only once by the EnVar and used in the ensemble LETKF analysis.

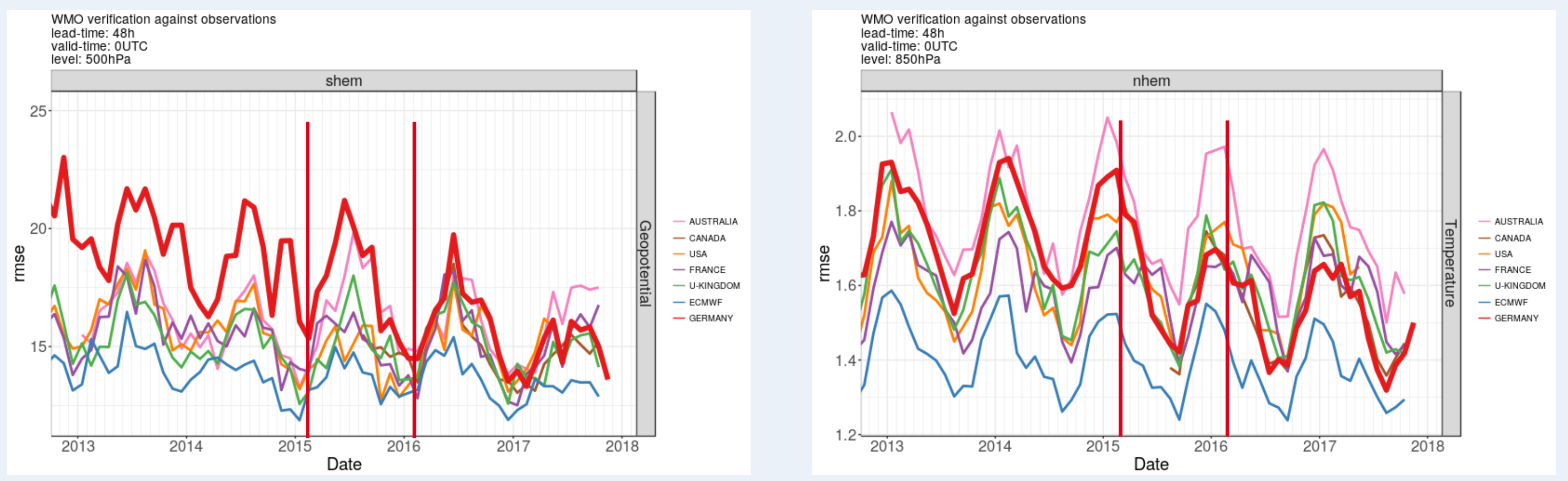

Fig 2: Evolution of DWD scores (thick red line) in comparison to a number of other global NWP centres for the years 2013 to present in the form of WMO comparison against radiosonde observations. Results vary depending on parameter, level and forecast lead time, but the improvements due to introduction of ICON and EnVAR+LETKF (vertical lines) are nearly always visible. Left: RMSE for geopotential, 500 hPa, SH; right: RMSE for temperature, 850 hPa, NH; both 48 h lead time.

4) High-resolution LETKF for **COSMO-DE,** operational since **March 2017**, using 40 members at 2.8 km resolution for a domain over Germany. It replaced the previous nudging scheme and also provides initial conditions for the **COSMO-EPS ensemble forecasts**. The LETKF enables the exploitation of additional remote sensing data. Ongoing work focuses on volume radar scans (3D forward operator implemented), GPS slant delays and cloud information and cloudy radiances from SEVIRI (METEOSAT) using both infrared (WV) and visible channels (**see VI**).

III) Introducing MW&IR humidity channels and MW-Imagers

Recent work has focused on introducing humidity radiances into the ICON EnVar+LETKF system. Previous work on this within the old GME model environment had not resulted in positive forecast impact. This was attributed to very strong interactions of the humidity information with the model physics, due to the model climate not being close enough to the observations. The tests have been resumed with the new NWP system, using MHS channels 3-5 from METOP and NOAA as well as 16 humidity channels from IASI over sea. Experiments have run for several months (winter and summer, 2016 and 2017). The IASI cloud detection uses the McNally&Watts (2003) scheme with WV channels flagged according to T-channels with similar height-ranking. The impact is consistently positive in terms of improved FG fit to observations as well as for forecast quality versus observations and analyses (Fig 3-6).

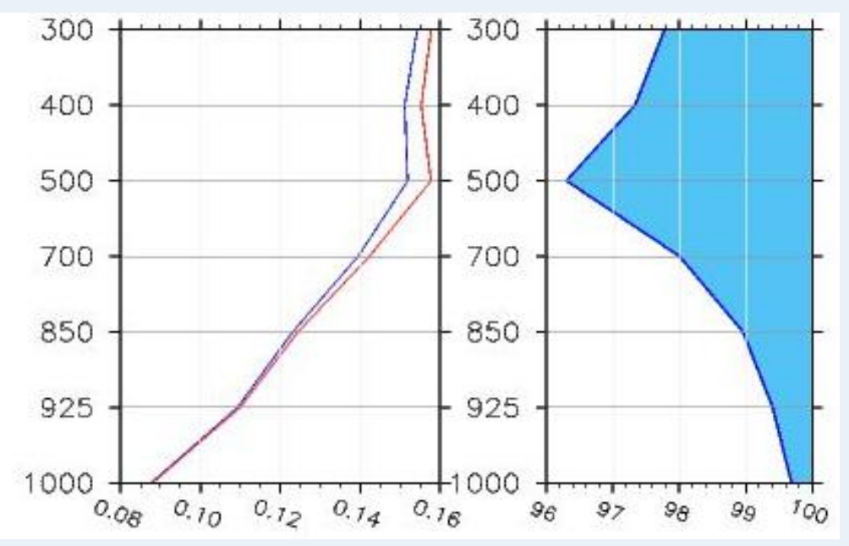

Fig 3: OBS-FG versus radiosondes for rel. humidity (Jul-Sep 17). Left: stdv for experiment (blue) and reference (red); right: rel. difference.

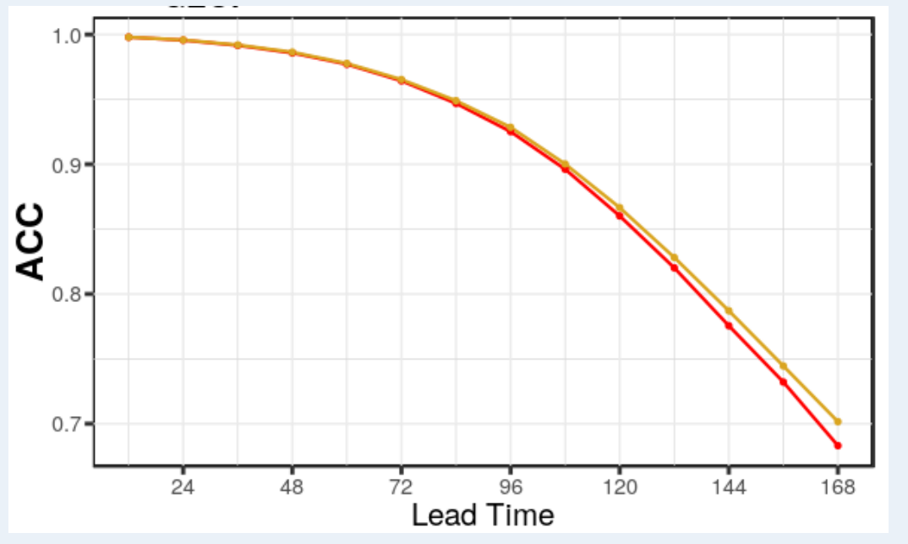

Fig 4: Anomaly correlation for 500 hPa geopotential (SH, Jul-Aug 17) for WV channel assimilation experiment (yellow), reference (red).

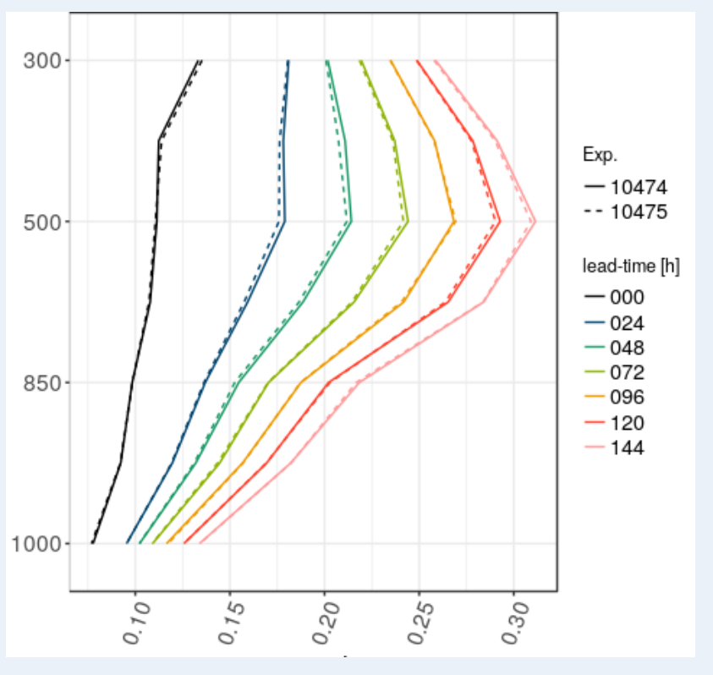

Fig 5: Radiosonde forecast verification (Aug-Sep 17). RMSE for rel. humidity.

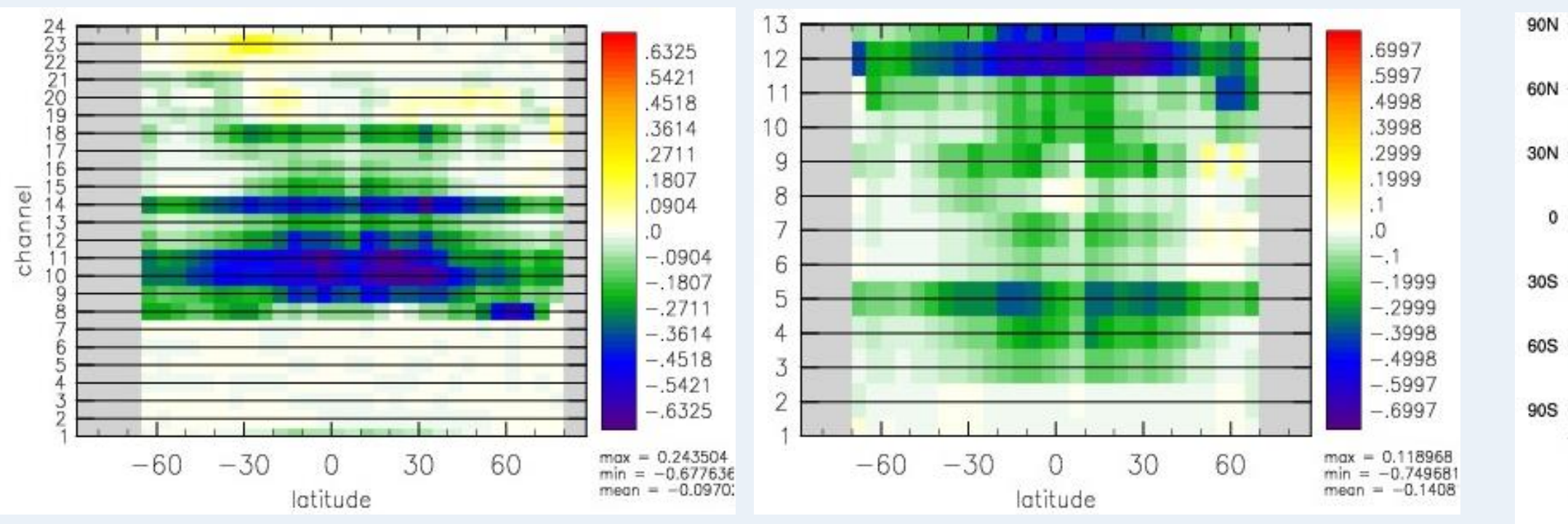

Fig 6: Difference of stdv(OBS-FG) between assimilation experiment and reference as zonal mean per channel. Left: SSMIS (ch 9-11:183 GHz band, ch 14: 22.2 GHz). Right: GMI (ch 12-13: 183 GHz band, ch5: 23.8 GHz).

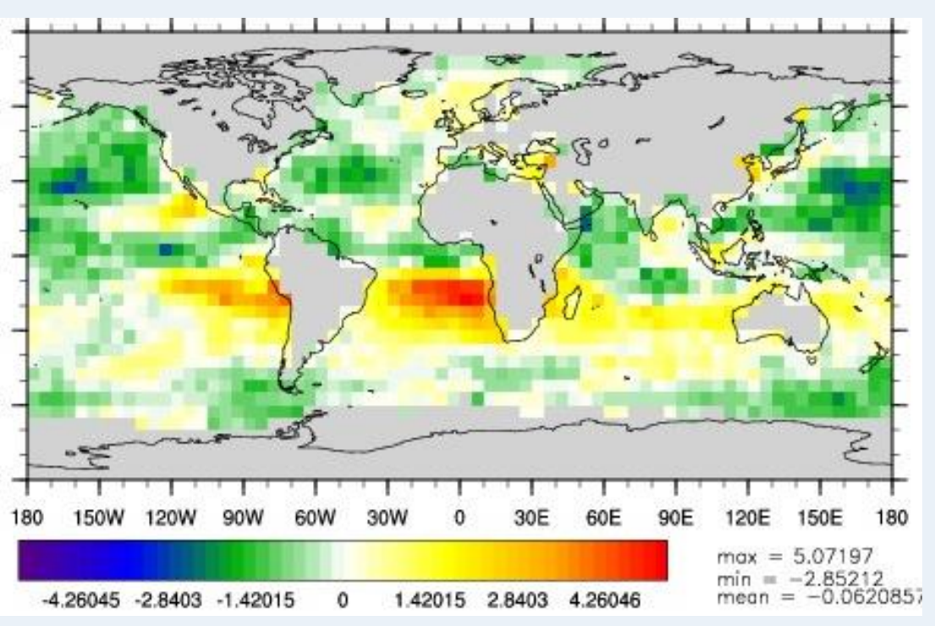

Fig 7: Mean OBS-FG for AMSR2 23.8 V used for model evaluation (May 2016).

Additional humidity sounders and imagers have also been technically implemented (ATMS, SSMIS, SAPHIR, GMI, AMSR-2) in a clear-sky context and are currently used for monitoring. The screening of cloud/precipitation affected radiances and also the bias correction are currently tuned further before moving on to assimilation tests with these data.

IV) MW & IR radiances over land

For extending the data usage over land to lower peaking channels, the use of the atlases provided with RTTOV-12 has been implemented (TELSEM2, CNRM for MW and UWIRemis for IR) and tested resulting in consistently improved OBS-FG fits for surface sensitive channels. Additionally, retrievals of surface emissivity ε_s are being studied: In the IR (IASI, CrIS), ε_s has been added to the state vector (containing also the skin temperature T_s) in the form of coefficients of a principal component (PC) representation of ε_s. Current work focuses on the estimation of the FG errors for T_s and PC coefficients and on improved (low) cloud detection over land (e.g. using AVHRR for IASI). For the MW, a direct retrieval using window channels is being tested following Prigent et al. (2005). Fig. 8 illustrates the changes in ε_s from a direct retrieval (using AMSU-A channel 3) and Fig. 9 the resulting improved OBS-FG fit (compared to CNRM atlas use) for the adjacent lowest sounding channel 4 using this ε_s .

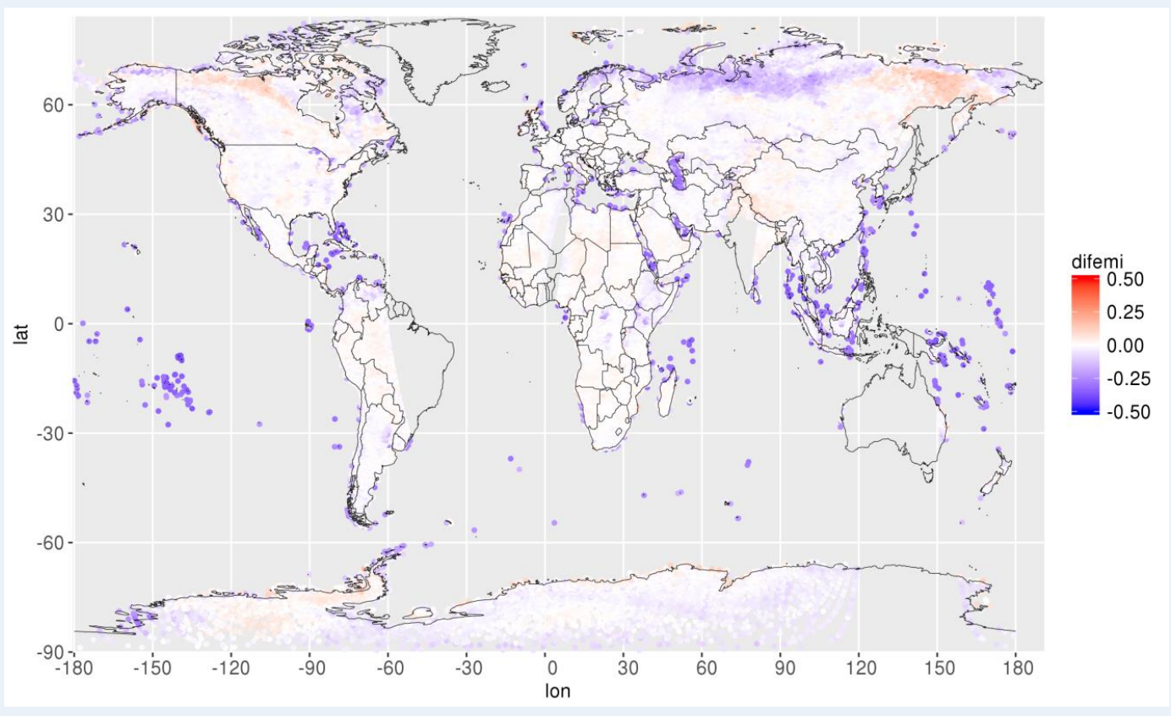

Fig 8: Difference of dynamically retrieved ε_s and CNRM atlas for AMSU-A channel 4 (1/5/2016, 3 UTC).

Fig 9 (right): pdf of OBS-FG for AMSU-A channel 4 using CNRM atlas (red) and dynamic retrieval (blue).

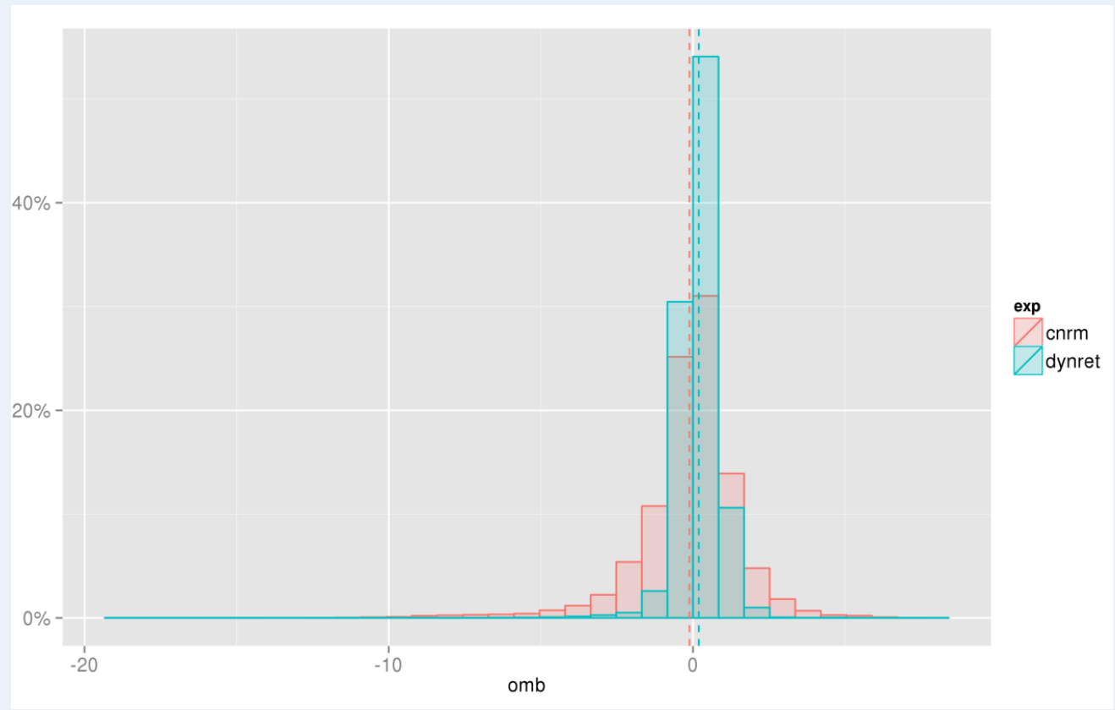

V) IASI PC compressed radiances

IASI principal component (PC) compressed data have been technically implemented. Initial experiments have been run assimilating PC data in the form of reconstructed radiances (RecRad) treating the RecRad like raw radiances in a first approach. A reduction in OBS-FG stdv can be seen for the temperature sensitive channels, attributed to reduced noise in the RecRad, which is not visible in the WV band having a much larger stdv of OBS-FG (Fig 10). Differences are also observed in cloud screening results with less clear data for most channels and marginally more for very high-peaking channels (Fig. 11). Forecast scores in assimilation are neutral to slightly positive.

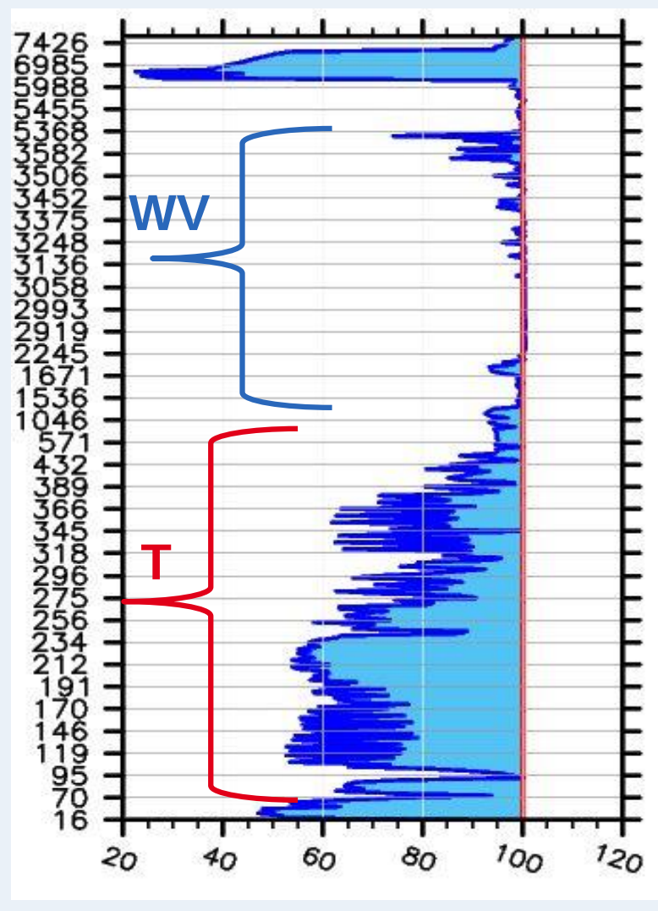

Fig 10: Relative difference of stdv of OBS-FG (in a monitoring setup) for RecRad experiment minus RawRad reference.

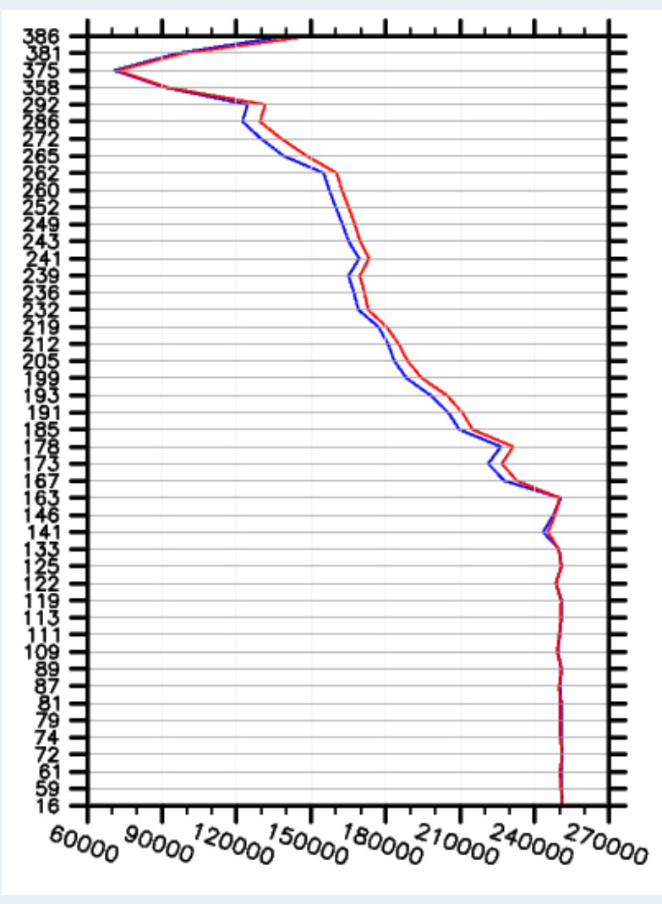

Fig 11: Difference of the number of RecRad (blue) and RawRad (red) observations flagged as clear in a monitoring setup.

VI) Towards the assimilation of SEVIRI visible reflectances in the high-resolution LETKF

For the convection-resolving KENDA system, projects are ongoing to assimilate cloudy IR radiances as well as visible reflectances to improve forecasts of convective events as well as of low level clouds (e.g. for renewable energy applications). The implementation of the fast forward operator MFASIS (Scheck et al., 2016) simulating SEVIRI visible channels is being evaluated and tuned using OBS-FG statistics (Fig. 12, 13). The fit to observed reflectances at high solar zenith angles improves when some 3D effects are accounted for. The water content of subgrid-scale clouds has to be taken into account, but including snow/graupel gives no further improvement. First assimilation studies with the KENDA LETKF (in cooperation with HErZ at LMU/Munich) are very promising, resulting in improved cloud cover and also better fit of humidity fields to independent observations (radiosonde, aircraft).

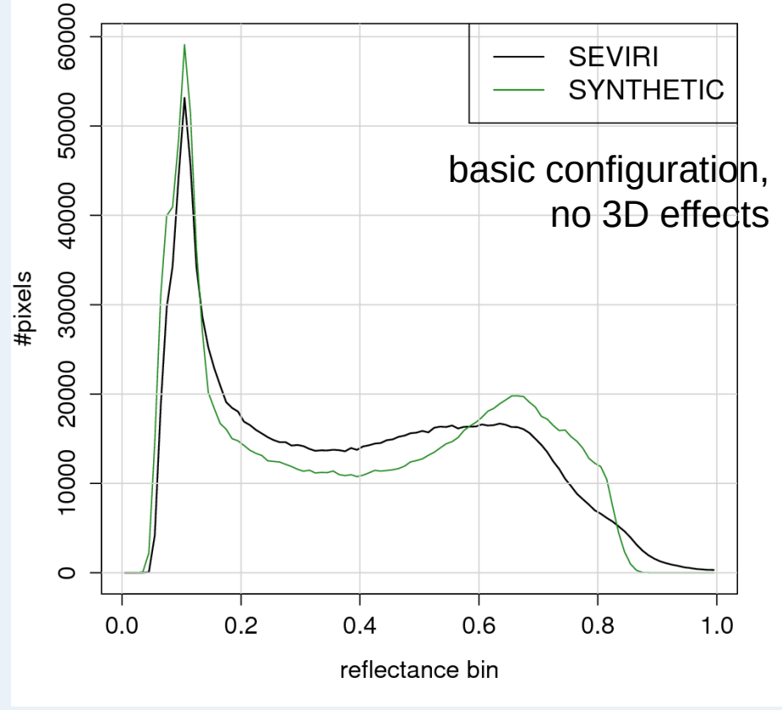

Fig 12: Histogram of SEVIRI 0.6 µm reflectance (black) and simulated values (green). COSMO model domain (12 UTC, 28 May to 6 June 2016).

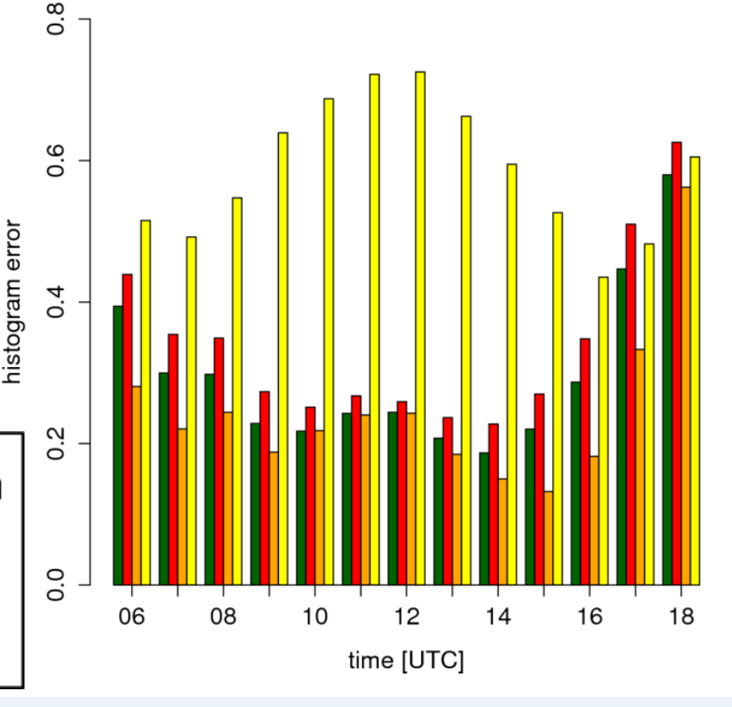

Fig 13: Average 0.6 µm reflectance histogram error as a function of time of day. Coloured bars show results for different configurations regarding MFASIS setup (3d-effects, orange) and the model to MFASIS interface (red, yellow, see legend).

Contact: Christina.Koepken-Watts@dwd.de, Data Assimilation Section, DWD (German Meteorological Service)

References:
Hunt, B.R., Kostelich, E.J, Szunyogh, I. 2007: Efficient data assimilation for spatiotemporal chaos: A local ensemble transform Kalman filter. *Physica D*, **230**, 112-126.
Prigent, C., Chevallier, F., Karbou, F., Bauer, P., Graeme K., 2005: AMSU-A Land Surface Emissivity Estimation for Numerical Weather Prediction Schemes, *J. Appl. Met.*, **44**, 416-426.
McNally, A. P. and Watts, P., 2003: A cloud detection algorithm for high-spectral-resolution infrared sounders. *Q. J. R. Met. Soc.*, **129,** 3411-3423.
Scheck L., Frèrebeau, P., Buras-Schnell, R., Mayer, B., 2016: A fast radiative transfer method for the simulation of visible satellite imagery. *J. Quant. Spectroscopy and Rad. Transfer*, **175**, 54-67.